Catalysis Communications 66 (2015) 30–33

Contents lists available at ScienceDirect

Catalysis Communications

journal homepage: www.elsevier.com/locate/catcom

Short communication

Synthesis of KOH/SnO_2 solid superbases for catalytic Knoevenagel condensation

Jun Xie, Lang Chen, Chak-Tong Au, Shuang-Feng Yin *

State Key Laboratory of Chemo/Biosensing and Chemometrics, College of Chemistry and Chemical Engineering, Hunan University, Changsha 410082, Hunan, China

ARTICLE INFO

Article history:
Received 24 December 2014
Received in revised form 27 February 2015
Accepted 7 March 2015
Available online 10 March 2015

Keywords:
KOH/SnO_2
Solid superbase
Graphene oxide
Knoevenagel condensation

ABSTRACT

KOH/SnO_2 solid superbases of specific morphology and uniform pore structure were synthesized. The SnO_2 support was prepared by reflux digestion using graphene oxide as template and employed for the loading of KOH by means of grinding and thermal treatment. With base strength of $26.5 \leq H_- < 33.0$ and superbasic sites of 1.362 mmol g^{-1}, the 20 wt.%KOH/SnO_2 catalyst exhibits excellent activity in Knoevenagel condensation under mild conditions. The catalytic efficiency is closely related to the base strength and the amount of superbasic sites. The findings disclose a new route for the synthesis of versatile solid superbases using SnO_2 as supports.

1. Introduction

Solid superbases are materials that possess basic sites with strength (H_-) higher than 26 [1]. In the past decades, there was rapid development in the research of solid superbase catalysts due to their excellent catalytic performance and environment-benign characteristics. Many superbases (e.g., $KNO_3/\gamma\text{-}Al_2O_3$ [2,3], $Eu_2O_3/\gamma\text{-}Al_2O_3$ [4], KNO_3/ZrO_2 [5,6], KOH/ZrO_2 [7], K/MgO [8], Na/NaOH/MgO [9], KNO_3/KL [10] and $Ca(NO_3)_2$/SBA-15 [11]) were reported. In these cases, the common supports are $\gamma\text{-}Al_2O_3$, ZrO_2, MgO and mesoporous molecular sieves. Obviously, due to the limited use of support materials, the variety of solid superbases is restricted. It is envisaged that the use of new support materials is a way to enrich the diversity of solid superbase materials. Previously, we synthesized a series of superbase materials using composite oxides as supports and potassium salts as modifying agents [12–14]. However, most of them show unsatisfactory catalytic performance that can be related to the poor amount of superbasic sites.

SnO_2 is not expensive. It has a fair amount of acidic sites, probably of weak acid strength [15]. It is chemically stable and is widely used in gas sensors [16], dye-based solar cells [17], transparent conducting electrodes [18], and catalyst supports [19]. It shows physical properties that are favorable for the formation of superbasic sites: high carrier mobility, rich crystal defects and abundant vacant sites [20,21]. Moreover, graphene oxide (GO) due to outstanding advantages such as low cost, easy availability, abundant surface functional groups, nontoxic nature, environmental friendliness and stability, has been recognized as the most promising and friendly material [22,23]. In the present work, we used SnO_2 prepared using GO template as support for the synthesis of superbases and investigated their catalytic activity towards the Knoevenagel condensation reaction under mild conditions.

2. Experimental

2.1. Catalyst preparation

SnO_2 was prepared by using graphene oxide as template under reflux digestion. $SnCl_4 \cdot 5H_2O$ (0.02 mol) was dissolved in deionized water, and 1 mol L^{-1} KOH aqueous solution was added dropwise with vigorous stirring until the pH value of the solution was 7. The solution was stirred at 40 °C for 3 h, followed by centrifugation and washing with water for 5 times to form a clear gel. The obtained gel was dissolved in water again, and mixed with an aqueous solution of 2 g L^{-1} GO synthesized by the modified Hummer's method [24]. The as-resulted mixture was digested under reflux at ca. 100 °C for 24 h, and the precipitate was filtered out. The obtained solid was dried at 110 °C overnight and calcined at 550 °C for 3 h to remove the GO template for the formation of SnO_2.

The KOH-loaded SnO_2 samples were prepared by grinding method, followed by thermal treatment at 550 °C under a flow of high-purity N_2 for 3 h. The as-prepared sample is denoted hereinafter as "xwt.%KOH/SnO_2", where x stands for the weight percentage of KOH in terms of the whole catalyst.

2.2. Catalyst characterization

XRD patterns were recorded on a Bruker D8 advance diffractometer with monochromatized Cu Kα radiation ($\lambda = 0.15406$ nm) at a setting

---

* Corresponding author.
E-mail address: sf_yin@hnu.edu.cn (S.-F. Yin).

http://dx.doi.org/10.1016/j.catcom.2015.03.008
1566-7367/

of 40 kV and 40 mA. SEM analyses were performed over a Hitachi S-4800 electron microscope operating at 2.0 kV. The specific surface areas of catalysts were determined by BET method based on nitrogen adsorption–desorption isotherms (at −196 °C) collected over a Beckman (SA 3100) surface area analyzer. The FT-IR spectra were determined using a Bruker vector 22 FT-IR spectrophotometer. The CO_2-TPD measurements were conducted on a Micromeritics 2920 apparatus using thermal conductivity detector. The sample was activated at 550 °C for 1 h prior to the adsorption of CO_2 at 100 °C. After purging at 100 °C to remove the physically adsorbed CO_2, the sample was heated to 800 °C at a rate of 10 °C min^{-1} and held at 800 °C for 40 min. The basicity of samples was measured using Hammett indicators after activation at 550 °C for 3 h as detailed in [25].

2.3. Catalyst evaluation

Catalytic activity of the superbases was investigated in the Knoevenagel condensation of aldehydes with active methylene compounds (Scheme S1, see the supporting information, SI). The catalytic reactions were conducted in a 25 mL round-bottomed flask at 25 °C using aldehyde (2 mmol), active methylene reagent (2 mmol), DMF (dimethylformamide, 1 mL), and catalyst (50 mg). After the reaction, the catalyst was separated from the mixture by centrifugation, and the reaction mixtures were analyzed using an Agilent Technologies 7820 gas chromatograph equipped with a flame ionization detector and AB-FFAP capillary column (30 m × 0.25 mm × 0.25 μm). The conversion of aldehydes and the yield of products were determined using biphenyl as internal standard. All the products were analyzed over an Agilent 6890-5973 MSD GC–MS equipment.

3. Results and discussion

3.1. Characterization results

3.1.1. XRD

Fig. S1 (SI) shows the XRD patterns of samples. In Fig. S1c, the SnO_2 sample prepared using GO template shows strong diffraction peaks at 2θ of 26.7, 34.1 and 51.7°, which are attributable to the SnO_2 phase (JCPDS no. 41-1445). There is no detection of additional peaks after the introduction of KOH up to a loading of 20 wt.%, indicating high dispersion of KOH on SnO_2. It is only at a KOH loading of 30 wt.% that there is the detection of signals attributable to KOH (JCPDS no. 21-645). Apparently, there exists a dispersion threshold of KOH on SnO_2, similar to the case of KNO_3 on zirconia [6] and the case of K_2CO_3 on alumina [26]. The spontaneous dispersion capacity of KOH on SnO_2 is around 20 wt.%. When KOH loading exceeds 20 wt.%, there is blocking of active sites and agglomeration of crystallites [12]. It is observed that the SnO_2 and 20 wt.% KOH/SnO_2 with SnO_2 prepared without using GO template (Fig. S1a, b) show sizes of 13.2 and 12.6 nm, respectively. On the other hand, the crystallite sizes of xwt.%KOH/SnO_2 (Fig. S1c–f) are estimated to be 10.0, 10.5, 11.1 and 9.9 nm at KOH loadings of 0, 10, 20 and 30 wt.%, respectively. The results demonstrate that the use of GO template leads to a decrease of crystallinity and an increase in the amount of defects [27].

3.1.2. SEM

Fig. 1 displays the SEM images of 20 wt.%KOH/SnO_2 prepared with or without the use of GO template. One can see that without the use of GO template for the preparation of SnO_2, the 20 wt.%KOH/SnO_2 is irregular in shape, and agglomeration is obvious. The use of GO as template for the preparation of SnO_2 leads to the formation of uniform nanoparticles with diameter of ca. 25 nm. We deduce that the basic precursors are anchored covalently to GO through functional groups such as carboxyl and hydroxyl [28]. Thus, the presence of GO template restrains agglomeration of nanoparticles, and shows important effect on the morphology of 20 wt.%KOH/SnO_2.

3.1.3. N_2 adsorption/desorption isotherm

Depicted in Fig. 2 are the N_2 adsorption/desorption isotherms and pore-size distribution of samples. One can see type-IV isotherms, and there are hysteresis loops that indicate mesoporosity of materials [3]. The BET surface area and pore volume of SnO_2 prepared using GO template are 39.1 $m^2\ g^{-1}$ and 0.137 $cm^3\ g^{-1}$, respectively. After the introduction of 20 wt.% KOH, there is a decline of BET surface area and pore volume (16.1 $m^2\ g^{-1}$ and 0.051 $cm^3\ g^{-1}$). Meanwhile, the pore-size distribution suggests uniform pore structure. In addition, the surface area and pore volume of SnO_2 prepared without using GO template are 21.7 $m^2\ g^{-1}$ and 0.111 $cm^3\ g^{-1}$, whereas those of 20 wt.%KOH/SnO_2 with SnO_2 prepared without using GO template are 10.0 $m^2\ g^{-1}$ and 0.034 $cm^3\ g^{-1}$, respectively. It is obvious that the use of GO template leads to increase of BET surface area and pore volume. It is deduced that GO promotes the dispersion while restraining the agglomeration of nanoparticles.

3.1.4. FT-IR

Shown in Fig. S2 (SI) are the IR spectra of as-synthesized SnO_2 and 20 wt.%KOH/SnO_2. The SnO_2 sample exhibits a strong band at 638 cm^{-1}, which is attributable to the anti-symmetric Sn–O–Sn stretching mode of surface-bridging oxide formed by condensation of adjacent surface hydroxyl groups. The band at 3420 cm^{-1} indicates the presence of hydroxyl groups, which is probably due to water adsorption [29]. After the introduction of KOH, there is the detection of the 1410 cm^{-1} band attributable to CO_3^{2-} vibration [30]. The presence of the 1410 cm^{-1} band demonstrates that the introduction of KOH promotes the formation of basic sites and the adsorption of CO_2 on the surface of SnO_2. To confirm the functional group on GO, we collected

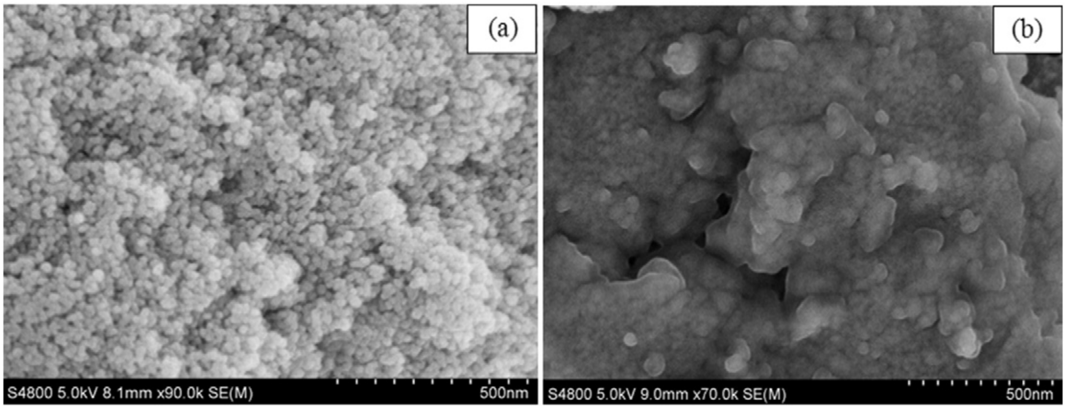

Fig. 1. SEM images of (a) 20 wt.%KOH/SnO_2 with SnO_2 prepared using GO template, and (b) 20 wt.%KOH/SnO_2 with SnO_2 prepared without using GO template.

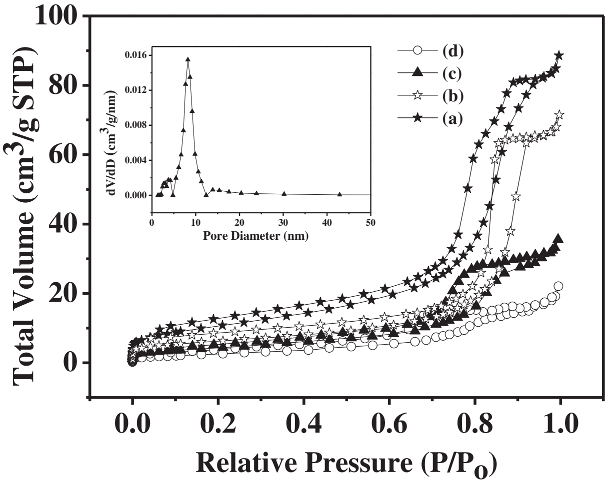

Fig. 2. N_2 adsorption/desorption isotherm of (a) SnO_2 prepared using GO template, (b) SnO_2 prepared without using GO template, (c) 20 wt.%KOH/SnO_2 with SnO_2 prepared using GO template, and (d) 20 wt.%KOH/SnO_2 with SnO_2 prepared without using GO template.

the IR spectrum of GO and compared it with that of GO treated with basic precursors (Fig. S3A, SI). The spectrum of GO showed absorption at 1720 cm^{-1} ascribable to C = O vibration of COOH [31]. However, this peak disappeared after GO was treated with basic precursors under reflux at ca. 100 °C for 24 h (Fig. S3B, SI), indicating that the basic precursors were anchored covalently to GO through the functional groups.

3.1.5. Hammett indicator method

The base strength (H_-) and basic sites of the samples were measured using Hammett indicators, and the effect of the KOH loading on the surface of SnO_2 was investigated. As shown in Table S1 (SI), the base strength of SnO_2 is $15.0 \leq H_- < 18.4$. From 0 to 20 wt.% KOH loading, there is a gradual rise of base strength. Having a superbasic strength of $26.5 \leq H_- < 33.0$, the 20 wt.%KOH/SnO_2 sample can be regarded as a solid superbase [1], and it shows an amount of superbasic sites of 1.362 mmol g^{-1}. With further increase of KOH loading, the amount of superbasic sites decreases while the base strength of samples remains at $26.5 \leq H_- < 33.0$. Therefore, to reach the highest possible amount of superbasic sites and to maintain excellence in base strength, a KOH loading of 20 wt.% should be adopted.

3.1.6. CO_2-TPD

The surface basicity of the samples was further estimated by the CO_2-TPD technique (Fig. 3). Without KOH loading, the SnO_2 sample prepared using GO as template shows CO_2 desorption peaks at ca. 126, 369, and 710 °C (Fig. 3c). With 20 wt.% KOH loading, desorption peaks are observed at ca. 134 and 798 °C (Fig. 3a). It is apparent that the KOH presence results in enhancement of CO_2 desorption and rise of desorption temperature. The desorption peaks at ca. 798 °C is a clear indication of superbasicity [30,32], and the amount of superbasic sites is 1.325 mmol g^{-1} calculated by the integral method based on the area of the corresponding desorption peaks. In other words, the introduction of KOH leads to obvious enhancement of basicity. As a control comparison, the 20 wt.%KOH/SnO_2 sample with SnO_2 prepared without the use of GO template shows CO_2 desorption amount and desorption temperature that are significantly lower (Fig. 3b). We deduce that the SnO_2 prepared using GO template has much more oxygen vacancies on the surface, which is favorable for the creation of superbasic sites. Despite the formation mechanism of superbasic sites needs further investigation, it is apparent that the use of GO template can improve the surface basicity of SnO_2.

3.2. Catalytic activity

3.2.1. Effect of KOH loading

Fig. 4a shows the effects of KOH loading on catalytic activity in the Knoevenagel condensation of benzaldehyde with ethyl cyanoacetate. The catalytic activity increases with increase of KOH loading, and reaches a maximum at 20 wt.%. Further increase of the KOH loading results in the decrease of the catalytic performance. It could be attributed to the agglomeration of catalyst particles and/or coverage of surface active sites caused by excess amount of KOH. Based on the results, the optimum KOH loading is 20 wt.%, in agreement with the results of XRD and Hammett indicator characterization. Furthermore, the influence of KOH loading on the basicity of KOH/SnO_2 was studied and the results are shown in Table S1 (SI) and Fig. 4b, it is obvious that the change of catalytic activity is not only related to the base strength but also to the amount of superbasic sites.

3.2.2. Knoevenagel condensation of various aldehydes with active methylene compounds

In order to test the applicability of 20 wt.%KOH/SnO_2, we studied the reaction of various aldehydes with methylene compounds having ethyl cyano acetate or malononitrile active group (Table 1). One can see product yields that are either comparable or superior to those reported in the

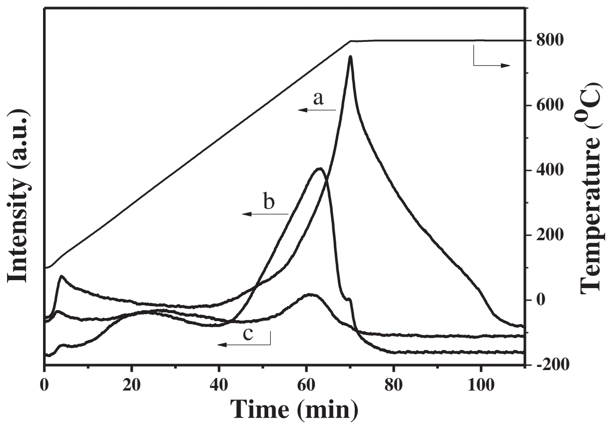

Fig. 3. CO_2-TPD profile of (a) 20 wt.%KOH/SnO_2 with SnO_2 prepared using GO template, (b) 20 wt.%KOH/SnO_2 with SnO_2 prepared without using GO template, and (c) SnO_2 prepared using GO template.

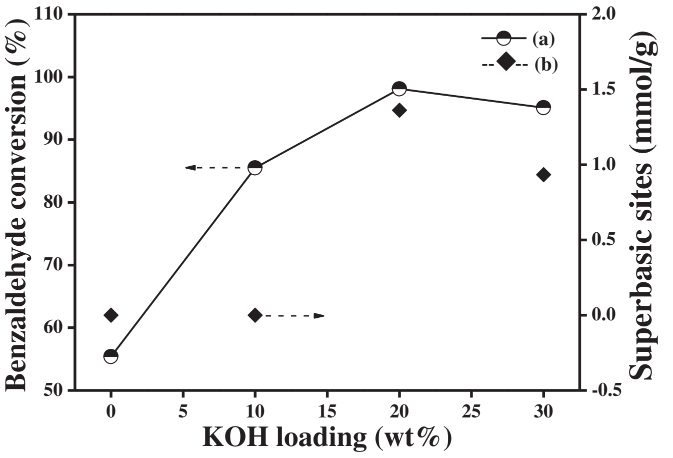

Fig. 4. Effects of KOH loading on benzaldehyde conversion and basicity. (Reaction conditions: benzaldehyde, 2 mmol; ethyl cyanoacetate, 2 mmol; DMF, 1 mL; catalyst, 50 mg; temperature, 25 °C; time, 15 min.)

Table 1
Knoevenagel condensation of various aldehydes with active methylene compounds over 20 wt.%KOH/SnO_2.

Entry	Aldehydes	Methylene compounds (R^2)	Yield (%)
1	Benzaldehyde	–CN	97.4
2	Benzaldehyde	–COOEt	98.1
3	4-Nitro Benzaldehyde	–CN	90.2
4	4-Nitro benzaldehyde	–COOEt	92.2
5	4-Chloro benzaldehyde	–CN	96.1
6	4-Chloro benzaldehyde	–COOEt	94.5
7	4-Methyl benzaldehyde	–CN	98.2
8	4-Methyl benzaldehyde	–COOEt	95.9
9	4-Methoxy benzaldehyde	–CN	92.8
10	4-Methoxy benzaldehyde	–COOEt	90.4

Reaction conditions: aldehyde, 2 mmol; active methylene compound, 2 mmol; DMF, 1 mL; catalyst, 50 mg; temperature, 25 °C; time, 15 min.

literature [12–14]. That is to say, the new solid superbase catalyst is a good alternative for Knoevenagel condensation reactions.

3.2.3. Catalyst recyclability

Recyclability of the catalyst for the Knoevenagel condensation of benzaldehyde with ethyl cyanoacetate was tested (Fig. S4, SI). After each cycle, the catalyst was separated from the product by centrifugation, and was immediately reused (with the addition of fresh reactants) without any treatment. There is an obvious decrease of product yield across the five cycles (from 98.1% to 90.3%), and the catalyst deactivation is likely due to the generation of H_2O that results in the loss of potassium species.

4. Conclusion

KOH/SnO_2 solid superbases with specific morphology and uniform pore structure were synthesized. We prepared the SnO_2 support by reflux digestion using graphene oxide as template. The use of GO template for the control of morphology results in high surface basicity. With a base strength of $26.5 \leq H_- < 33.0$ and an amount of superbasic sites up to 1.362 mmol g^{-1}, the 20 wt.%KOH/SnO_2 catalyst shows excellent catalytic activity towards the Knoevenagel condensation reaction under mild conditions. Our findings disclose a new route for the use of SnO_2 as support in the synthesis of versatile solid superbases.

Acknowledgments

The project was financially supported by the National Natural Science Foundation of China (Grant Nos. U1162109, 21273067, 21401054 and 21476065), Program for Changjiang Scholars and Innovative Research Team in University (IRT1238), and the Fundamental Research Funds for the Central Universities. C.T. Au thanks the Hunan University for an adjunct professorship.

Appendix A. Supplementary data

Supplementary data to this article can be found online at http://dx.doi.org/10.1016/j.catcom.2015.03.008.

References

[1] K. Tanabe, M. Misono, Y. Ono, H. Hattori, New Solid Acids and Bases, Their Catalytic Properties, Kodansha, Tokyo, 1989. 3.
[2] J.H. Zhu, Y. Wang, Y. Chun, X.S. Wang, J. Chem. Soc. Faraday Trans. 94 (1998) 1163–1169.
[3] L.B. Sun, J. Yang, J.H. Kou, F.N. Gu, Y. Chun, Y. Wang, J.H. Zhu, Z.G. Zou, Angew. Chem. Int. Ed. 47 (2008) 3418–3421.
[4] X. Li, G.Z. Lu, Y.L. Guo, Y. Guo, Y.Q. Wang, Z.G. Zhang, X.H. Liu, Y.S. Wang, Catal. Commun. 8 (2007) 1969–1972.
[5] Y. Wang, W.Y. Huang, Z. Wu, Y. Chun, J.H. Zhu, Mater. Lett. 46 (2000) 198–204.
[6] Y. Wang, W.Y. Huang, Y. Chun, J.R. Xia, J.H. Zhu, Chem. Mater. 13 (2001) 670–677.
[7] S.F. Yin, B.Q. Xu, S.J. Wang, C.T. Au, Appl. Catal. A Gen. 301 (2006) 202–210.
[8] A.M. Ferrari, G. Pacchioni, J. Phys. Chem. 99 (1995) 17010–17018.
[9] N.J. Sun, K.J. Klabunde, J. Catal. 185 (1999) 506–512.
[10] J.H. Zhu, Y. Chun, Y. Wang, Q.H. Xu, Mater. Lett. 33 (1997) 207–210.
[11] L.B. Sun, J.H. Kou, Y. Chun, J. Yang, F.N. Gu, Y. Wang, J.H. Zhu, Z.G. Zou, Inorg. Chem. 47 (2008) 4199–4208.
[12] Y.D. Wei, S.G. Zhang, S.F. Yin, S.L. Luo, C.T. Au, Catal. Commun. 12 (2011) 1333–1338.
[13] J. Zhao, J. Xie, C.T. Au, S.F. Yin, Appl. Catal. A Gen. 400 (2013) 61–69.
[14] J. Zhao, J. Xie, C.T. Au, S.F. Yin, RSC Adv. 4 (2014) 6159–6164.
[15] M. Ai, J. Catal. 4 (1975) 318–326.
[16] X.M. Zhou, W.Y. Fu, H.B. Yang, Y.Y. Zhang, M.H. Li, Y.X. Li, Mater. Lett. 90 (2013) 53–55.
[17] X.C. Dou, D. Sabba, N. Mathews, L.H. Wong, Y.M. Lam, S. Mhaisalkar, Chem. Mater. 23 (2011) 3938–3945.
[18] Y.S. He, J.C. Campbell, R.C. Murphy, M.F. Arendt, J.S. Swinnea, J. Mater. Res. 8 (1993) 3131–3134.
[19] D.Z. Wang, S.L. Wen, J. Chen, S.Y. Zhang, F.Q. Li, Phys. Rev. B 49 (1994) 14282.
[20] K.G. Godinho, A. Walsh, G.W. Watson, J. Phys. Chem. C 113 (2009) 439–448.
[21] H.T. Chen, S.J. Xiong, X.L. Wu, J. Zhu, J.C. Shen, Nano Lett. 9 (2009) 1926–1931.
[22] P.V. Kamat, J. Phys. Chem. Lett. 1 (2010) 520–527.
[23] Z.Y. Lu, J.X. Zhu, D.H. Sim, W.W. Zhou, W.H. Shi, Q.Y. Yan, Chem. Mater. 23 (2011) 5293–5295.
[24] D.C. Marcano, D.V. Kosynkin, J.M. Berlin, A. Sinitskii, Z.Z. Sun, A. Slesarev, L.B. Alemany, W. Lu, J.M. Tour, ACS Nano 4 (2010) 4806–4814.
[25] S.G. Zhang, Y.D. Wei, S.F. Yin, C.T. Au, Catal. Commun. 12 (2011) 712–716.
[26] Y. Wang, J.H. Zhu, W.Y. Huang, Phys. Chem. Chem. Phys. 3 (2001) 2537–2543.
[27] R. Shi, G.L. Huang, J. Lin, Y.F. Zhu, J. Phys. Chem. C 113 (2009) 19633–19638.
[28] H.L. Wang, L.F. Cui, Y. Yang, H.S. Casalongue, J.T. Robinson, Y.Y. Liang, Y. Cui, H.J. Dai, J. Am. Chem. Soc. 132 (2010) 13978–13980.
[29] F. Gu, S.F. Wang, C.F. Song, M.K. Lü, Y.X. Qi, G.J. Zhou, D. Xu, D.R. Yuan, Chem. Phys. Lett. 372 (2003) 451–454.
[30] T.T. Li, L.B. Sun, L. Gong, X.Y. Liu, X.Q. Liu, J. Mol. Catal. A Chem. 352 (2012) 38–44.
[31] X.B. Liu, P.B. Shang, Y.B. Zhang, X.L. Wang, Z.M. Fan, B.X. Wang, Y.Y. Zheng, J. Mater. Chem. A 2 (2014) 15273–15278.
[32] S.G. Zhang, Y.D. Wei, S.F. Yin, S.L. Luo, C.T. Au, Appl. Catal. A Gen. 406 (2011) 113–118.